Modern Physics Letters B
Vol. 28, No. 15 (2014) 1450117 (10 pages)

DOI: 10.1142/S0217984914501176

Controllable optical steady behavior from nonradiative coherence in GaAs quantum well driven by a single elliptically polarized field

Zhonghu Zhu*, Ai-Xi Chen†, Yanfeng Bai*, Wen-Xing Yang*,§ and Ray-Kuang Lee‡

*Department of Physics, Southeast University, Nanjing 210096, China
†Department of Applied Physics, School of Basic Science,
East China Jiaotong University, Nanchang 330013, China
‡Institute of Photonics Technologies,
National Tsing-Hua University, Hsinchu 300, Taiwan
§wenxingyang@seu.edu.cn

Received 16 March 2014
Revised 21 April 2014
Accepted 7 May 2014
Published 23 May 2014

In this paper, we analyze theoretically the optical steady behavior in GaAs quantum well structure which interacts with a single elliptically polarized field (EPF) and a π-polarized probe field. Due to the existence of the robust nonradiative coherence, we demonstrate that the controllable optical steady behavior including multi-stability (OM) and optical bistability (OB) can be obtained. More interestingly, our numerical results also illustrate that tuning the phase difference between two components of polarized electric field of the EPF can realize the conversion between OB and OM. Our results illustrate the potential to utilize the optical phase for developing the new all-optical switching devices, as well as a guidance in the design for possible experimental implementations.

Keywords: Semiconductor quantum well; optical bistability and multistability; nonradiative coherence; elliptically polarized field.

PACS Number(s): 78.67.De, 42.65.Pc, 42.50.Gy

Controlling optical steady behavior is the subject of active research over the past decade in view of its potential applications in optical devices, quantum information and so on. An interesting problem in this area is the creation of controllable optical bistability (OB) and multi-stability (OM).[1–19] As shown in Fig. 1, we take OB curve as an example to discuss the basic process of the input–output light intensity. Along the OA line, the output light intensity I_T increases progressively with gradual increasing of the input light intensity I_i. However, when I_i increases and reaches to I_B, I_T increases and reaches to I'_C nonlinearly. Consequently, I_T linearly increases along the CE line, which means that the absorption of the input light has reached saturation. If the I_i decreases from point E, I_T will linearly reduce along the EC line.

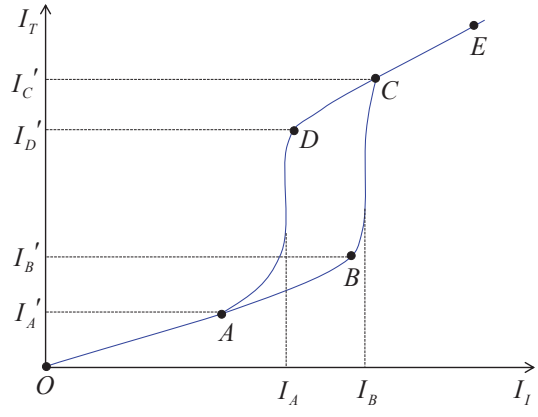

Fig. 1. (Color online) The diagrammatic sketch of the optical bistability.

When I_i decreases and reaches to I_B, I_T will linearly decrease along the ECD curve. In addition, if I_i decreases to I_A, I_T will nonlinearly decrease to I'_A accordingly, then I_T will linearly decrease along the AO line. In other words, for a certain input light intensity, there are two stable states of the output light intensity (i.e. the higher transmission state and the lower transmission state).

It is worth noting that stability refers to the output light intensity which is only the nonlinear function of the input light intensity that does not change over time. The schemes for obtaining controllable OB or OM have been proposed and observed theoretically and experimentally in several atomic system.[1–19] These studies mainly focused on controlling the bistable behaviors consisting of the bistable threshold and the shape of the bistable curve via quantum interference and atomic coherence.[1–19] It is worth noting that the creations of controllable OB or OM in semiconductor quantum wells (SQW) based on quantum coherence with intersubband transitions (ISBT) have also attracted an increasing number of interest[20–23] because of its wide applications in solid-state quantum information science and optoelectronics.[24–35]

On the other hand, recent studies of spin control in SQW found that nonradiative coherence is very robust and can be sustained for long time at room temperature.[36–43] The ISBTs in the SQW system can be described as $|S_z = \pm 1/2\rangle \leftrightarrow |J_z = \pm 1/2, \pm 3/2\rangle$ with $|S_z = \pm 1/2\rangle$ the conduction bands and $|J_z = \pm 1/2, \pm 3/2\rangle$ the light-hole (lh) and heavy-hole (hh) valence bands. Li *et al.*[44] realized electromagnetically induced transparency in the similar SQW system where we could observe the robust nonradiative coherence. Yang *et al.*[45] investigated the four-wave mixing in a double-V scheme via nonradiative coherence. Recently, Liu *et al.*[46] studied the properties of the soliton pairs with slow group velocity in SQW, which showed that the nonradiative coherence can effectively modify the propagation of soliton. However, there is not the related experimental study which has realized OM and OB via nonradiative coherence in current system, which motivates our study.

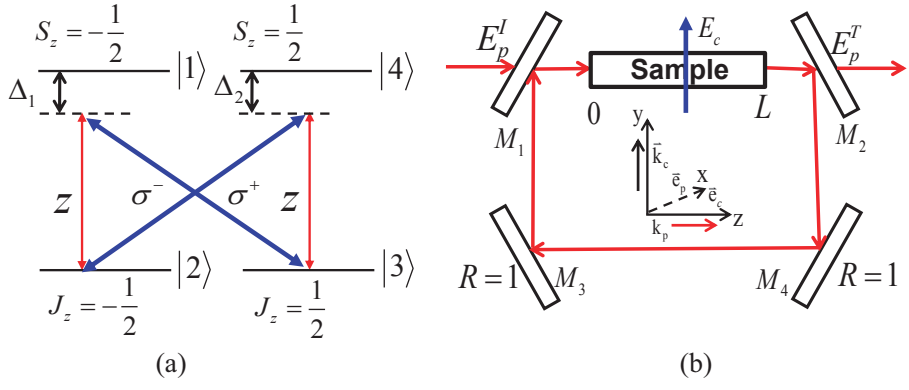

Fig. 2. (Color online) (a) Structure of GaAs quantum well system. The transitions between the states $|1\rangle$ and $|3\rangle$, and between the states $|2\rangle$ and $|4\rangle$ are driven by an elliptically polarized field (EPF). The transitions between the states $|1\rangle$ and $|2\rangle$, and between the states $|3\rangle$ and $|4\rangle$ are driven by a π-polarized probe field. The frequency detunings of system are correspondingly defined by Δ_1 and Δ_2. (b) Schematic diagram of the optical cavity containing a SQW sample of length L, where the control field E_c is noncirculating inside the cavity. E_p^T and E_p^I are the transmitted and incident fields, respectively. The two polarized fields both propagate along the y-axis in the QW waveguide.

In this paper, a new scheme which is aimed at the realization of controllable OB and OM via the nonradiative coherence in SQW is put forward. As shown in Fig. 2(a), the probe field E_p (with angular frequency ω_p) couples the electric dipole transitions between the levels $|1\rangle$ and $|2\rangle$ (with transition frequency ω_{21}), and between the levels $|3\rangle$ and $|4\rangle$ (with transition frequency ω_{43}). A single elliptically polarized field (EPF) E_c (with angular frequency ω_c) drives the electric dipole transitions between the levels $|1\rangle$ and $|3\rangle$ (with transition frequency ω_{31}), and between the levels $|2\rangle$ and $|4\rangle$ (with transition frequency ω_{42}). As shown in Fig. 2(b), we use the control beam which polarizes along the x-direction and the probe beam which polarizes along the z-direction. Both the two fields propagate along the y-axis in the SQW sample and drive the respective lh transitions.

We should note that the nonradiative coherence origins from the two lh valence bands can be neglected since the decoherence time is very short.[36–43] The utilization of a quarter-wave plate (QWP) can obtain the σ-polarization of the EPF.[47] An initial σ-polarized field E_c with a rotating angle ϕ can be elliptically polarized after entering into the QWP. Thus, the EPF can be decomposed as $E_c = E_c^+\sigma^+ + E_c^-\sigma^-$ with the unit basis vectors σ^- and σ^+, where $E_c^+ = \frac{E_c}{\sqrt{2}}(\cos\phi + \sin\phi)e^{i\phi}$ and $E_c^- = \frac{E_c}{\sqrt{2}}(\cos\phi - \sin\phi)e^{-i\phi}$. The amplitudes and the phase difference between two components of polarized electric field which is denoted by the rotating angle ϕ for convenience can be modulated by the QWP.

By choosing the $H_0 = \omega_p|2\rangle\langle 2| + \omega_c|3\rangle\langle 3| + (\omega_p + \omega_c)|4\rangle\langle 4|$ and taking the level $|1\rangle$ as the energy origin, under the dipole and rotating-wave approximation, the

interaction Hamiltonian of the present SQW structure is given by ($\hbar = 1$):

$$H_{\rm int} = \Delta_1|2\rangle\langle 2| + \Delta_1|3\rangle\langle 3| + (\Delta_1 + \Delta_2)|4\rangle\langle 4| - [\Omega_p|2\rangle\langle 1| + \Omega_p|4\rangle\langle 3| + \Omega_{c1}(\cos\phi - \sin\phi)e^{-i\phi}|3\rangle\langle 1| + \Omega_{c2}(\cos\phi + \sin\phi)e^{i\phi}|4\rangle\langle 2| + \text{H.c.}]\,, \quad (1)$$

where $\Delta_1 = \omega_{21} - \omega_p = \omega_{31} - \omega_c$ and $\Delta_2 = \omega_{43} - \omega_p = \omega_{42} - \omega_c$ are the relevant frequency detunings. The symbol H.c. means the Hermitian conjugation. $\Omega_{c1} = -\mu_{31}E_c^-/\hbar = \Omega_c(\cos\phi - \sin\phi)e^{-i\phi}$ and $\Omega_{c2} = -\mu_{42}E_c^+/\hbar = \Omega_c(\cos\phi + \sin\phi)e^{i\phi}$ are the half Rabi frequencies of the two components of the EPF, where $\Omega_c = -\mu E_c/\sqrt{2}\hbar$. $\Omega_p = \mu E_p/2\hbar$ is the half Rabi frequency of the probe field with $\mu_{ij} = \mu$ denoting the dipole matrix moment for the relevant optical transition from the level $|i\rangle$ to the level $|j\rangle$. Then, the density-matrix equations of system can be obtained under the standard approaches:[48–50]

$$\dot{\rho}_{22} = \gamma_{42}\rho_{44} + i\Omega_p\rho_{12} - i\Omega_p^*\rho_{21} + i\Omega_{c2}^*(\cos\phi + \sin\phi)e^{-i\phi}\rho_{42} - i\Omega_{c2}(\cos\phi + \sin\phi)e^{i\phi}\rho_{24}\,, \quad (2)$$

$$\dot{\rho}_{33} = \gamma_{43}\rho_{44} + i\Omega_p^*\rho_{43} - i\Omega_p\rho_{34} + i\Omega_{c1}(\cos\phi - \sin\phi)e^{-i\phi}\rho_{13} - i\Omega_{c1}^*(\cos\phi - \sin\phi)e^{i\phi}\rho_{31}\,, \quad (3)$$

$$\dot{\rho}_{44} = -(\gamma_{43} + \gamma_{42})\rho_{44} + i\Omega_p\rho_{34} - i\Omega_p^*\rho_{43} + i\Omega_{c2}(\cos\phi + \sin\phi)e^{i\phi}\rho_{24} - i\Omega_{c2}^*(\cos\phi + \sin\phi)e^{-i\phi}\rho_{42}\,, \quad (4)$$

$$\dot{\rho}_{21} = (-i\Delta_1 - \gamma_{21}/2)\rho_{21} - i\Omega_{c1}(\cos\phi - \sin\phi)e^{-i\phi}\rho_{23} + i\Omega_p(\rho_{11} - \rho_{22}) + i\Omega_{c2}^*(\cos\phi + \sin\phi)e^{-i\phi}\rho_{41}\,, \quad (5)$$

$$\dot{\rho}_{31} = -(i\Delta_1 + \gamma_{31}/2)\rho_{31} - i\Omega_p\rho_{32} + i\Omega_p^*\rho_{41} + i\Omega_{c1}(\cos\phi - \sin\phi)e^{-i\phi}(\rho_{11} - \rho_{33})\,, \quad (6)$$

$$\dot{\rho}_{41} = [-i(\Delta_1 + \Delta_2) - (\gamma_{43} + \gamma_{42})/2]\rho_{41} - i\Omega_p\rho_{42} + i\Omega_{c2}(\cos\phi + \sin\phi)e^{i\phi}\rho_{21} + i\Omega_p\rho_{31} - i\Omega_{c1}(\cos\phi - \sin\phi)e^{-i\phi}\rho_{43}\,, \quad (7)$$

$$\dot{\rho}_{42} = [-i\Delta_2 - (\gamma_{43} + \gamma_{42} + \gamma_{21})/2]\rho_{42} - i\Omega_p^*\rho_{41} + i\Omega_{c2}(\cos\phi + \sin\phi)e^{i\phi}(\rho_{22} - \rho_{44}) + i\Omega_p\rho_{32}, \quad (8)$$

$$\dot{\rho}_{43} = [-i\Delta_2 - (\gamma_{43} + \gamma_{42} + \gamma_{21})/2]\rho_{43} - i\Omega_{c1}^*(\cos\phi - \sin\phi)e^{i\phi}\rho_{41} + i\Omega_p(\rho_{33} - \rho_{44}) + i\Omega_{c2}(\cos\phi + \sin\phi)e^{i\phi}\rho_{23}, \quad (9)$$

$$\dot{\rho}_{32} = -[(\gamma_{21} + \gamma_{31})/2]\rho_{32} + i\Omega_{c1}(\cos\phi - \sin\phi)e^{-i\phi}\rho_{12} - i\Omega_{c2}(\cos\phi + \sin\phi)e^{i\phi}\rho_{34} - i\Omega_p^*\rho_{31} + i\Omega_p^*\rho_{42} \quad (10)$$

together with $\rho_{ji} = \rho_{ij}^*$ and $\sum_{j=1}^4 \rho_{jj} = 1$, where the total decay rates of the above density matrix equations which are added phenomenologically are denoted by γ_{ij} $(i, j = 1 - 4)$.[27–30]

To create controllable OB or OM, as shown in Fig. 2(b), the above-described SQW sample is put in a optical cavity of length L. For simplicity, a standard model is adopted, it is assumed that both the mirrors M_3 and M_4 have 100% reflectivity, and T and R (with $T+R=1$) are corresponding the intensity transmission and reflection coefficients of the mirrors M_2 and M_1, respectively. Only the probe field E_p which is determined by Maxwell's equation circulates inside an optical cavity, and then under the slowly varying envelope approximation, we can obtain the relevant propagating equation characterizing the probe field

$$\frac{\partial E_p}{\partial t} + c\frac{\partial E_p}{\partial z} = i\frac{\omega_p}{2\varepsilon_0}P(\omega_p)\,, \tag{11}$$

where the parameters c and ε_0 are the light speed in vacuum and the permittivity of free space, respectively. $P(\omega_p) = N(\mu_{12}\rho_{12} + \mu_{34}\rho_{34})$ denotes the slowly oscillating term of induce polarization in the relevant transitions $|1\rangle \leftrightarrow |2\rangle$ and $|3\rangle \leftrightarrow |4\rangle$ with N the electron number density in the conduction band of the SQW sample. In the steady-state condition, the time derivative $\partial E_p/\partial t$ in Eq. (11) can be neglected, thus the amplitude of the probe field E_p can be described by

$$\frac{\partial E_p}{\partial z} = i\frac{\omega_p}{2c\varepsilon_0}P(\omega_p)\,. \tag{12}$$

Note that if a set of reasonable parameters of the ring cavity can be found, the input field E_p^I and the transmitted field E_p^T will meet the conditions:[51,52]

$$E_p^T = \sqrt{T}E_p(L)\,, \tag{13}$$

$$E_p(0) = \sqrt{T}E_p^I(L) + RE_p(L)\,, \tag{14}$$

where the term $RE_p(L)$ in Eq. (14) presents a feedback mechanism results from the reflection of the mirror M_2 and is the main reason leads to OB or OM. By normalizing the fields ($x = \mu_{12}E_p^T/\hbar\sqrt{T}$ and $y = \mu_{12}E_p^I/\hbar\sqrt{T}$) and using the mean-field approximation,[51,52] the input–output relationship equation can be described by

$$y = x - iC[\rho_{12} + (\mu_{34}/\mu_{12})\rho_{34}]\,, \tag{15}$$

where $C = \frac{LN\omega_p\mu_{12}^2}{2\hbar c\varepsilon_0 T}$ is the electronic cooperation parameter. We should note that the term $iC[\rho_{12} + (\mu_{34}/\mu_{12})\rho_{34}]$ in Eq. (15) is very important for the OB or OM to occur.

In the following, we will directly examine the steady behavior of the output field by numerically integrating equations (2)–(10) in the steady-state condition (i.e. $\partial\rho_{ij} = 0$). For a qualitative analysis of the optical steady behavior, we take $\gamma_{42} = \gamma_{43} = \gamma = 10^{12}\ \mathrm{s}^{-1}$, $\gamma_{21} = \gamma_{31} = 1.5\gamma$.[44] Without loss of generality, taking $\Delta_1 = \Delta_2$, $\Omega_{c1} = \Omega_{c2} = \Omega_c$, $\mu_{24} = \mu_{13}$ and $\mu_{12} = \mu_{34}$, all the parameters used in the following numerical calculations are in the unit of γ. Besides, it is assumed that the Rabi frequencies Ω_p is real. Subsequently, as shown in Figs. 3–5, we obtain a few numerical results for the steady behavior of the input–output field intensity with

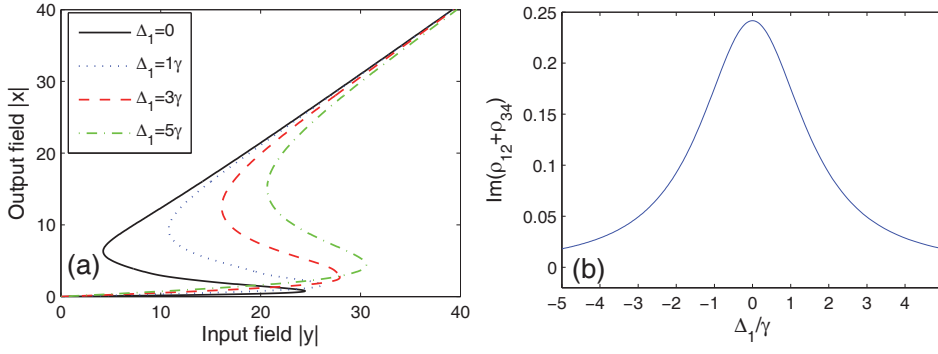

Fig. 3. (Color online) (a) The curve diagrams of the input–output field intensity with different frequency detuning Δ_1. (b) The probe absorption $\mathrm{Im}(\rho_{12} + \rho_{34})$ versus the detuning Δ_1 with $\Omega_p = \Omega_p^* = 0.5\gamma$. Other values of the parameters are chosen as $\Omega_c = 3\gamma$, $C = 100\gamma$ and $\phi = 0$.

different values of the relevant parameters to illustrate that controllable OB and OM can be achieved in the present SQW system.

First of all, we show in Fig. 3(a) the curve diagrams of the input–output field intensity with different frequency detuning Δ_1, in which the OB behavior can be obviously observed and can be manipulated by the frequency detuning. From Fig. 3(a), it is shown that the bistable threshold and the area of the bistable curve are controllable via changing the frequency detuning Δ_1. We can see, with increasing Δ_1 from 0 to 5γ, the bistable threshold increases progressively and the area of the bistable curve becomes wider when all other parameters keep fixed. The physics mechanism is rather clear and can be qualitatively explained as follows. The nonradiative coherence ρ_{14} results from the two transition pathways, i.e., $|2\rangle \leftrightarrow |1\rangle$ and $|2\rangle \leftrightarrow |4\rangle$, which can be modulated by the σ^+ polarized component of the EPF via the transition pathway $|2\rangle \leftrightarrow |4\rangle$. The absorption–dispersion property of the probe field coupled to the transition $|1\rangle \leftrightarrow |2\rangle$ is similar as the case of the usual electromagnetically induced transparency in a single V-type system.[43] However, here the nonradiative coherence ρ_{14} can also be induced by the σ^- polarized component of the control field via the transition pathway $|3\rangle \leftrightarrow |1\rangle$, which leads to the change of the absorption–dispersion property of the probe field corresponding to the transition $|3\rangle \leftrightarrow |4\rangle$. Thus, it is illustrated that the absorption–dispersion of the probe field can be modified in the present SQW system. The probe absorption $\mathrm{Im}(\rho_{12} + \rho_{34})$ versus the detuning Δ_1 is shown in Fig. 3(b), which displays the absorption of the probe field on the transitions $|1\rangle \leftrightarrow |2\rangle$ and $|3\rangle \leftrightarrow |4\rangle$. As illustrated in Fig. 3(b), the absorption of the probe field decreases accordingly with gradual increasing Δ_1 from 0 to 5γ. Thus, it is difficult for the absorption saturation of the ring cavity. Therefore, the OB behavior in Fig. 3(a) shows to be controllable when changing Δ_1. Furthermore, we can change the resonance conditions of the field via giving a time-modulated detuning.[27] As a result, we provide a scheme for controlling OB behavior via adjusting properly detuning in the SQW system.

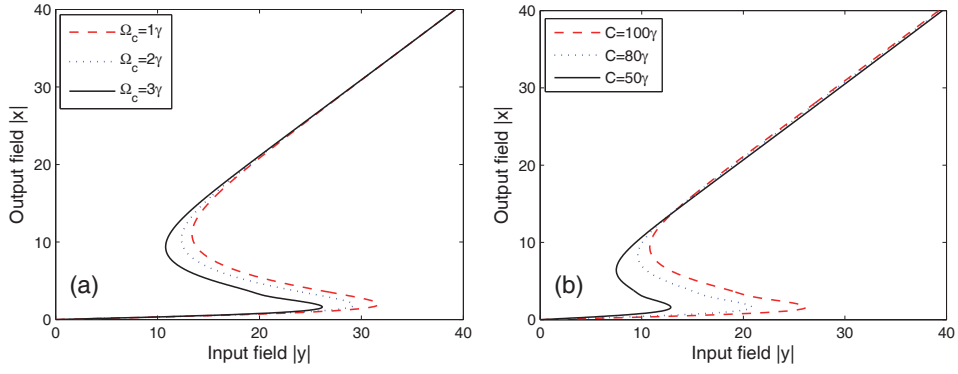

Fig. 4. (Color online) The curve diagrams of the input–output field intensity (a) with different intensity of the elliptically polarized field Ω_c with $C = 100\gamma$, (b) with different cooperation parameter C with $\Omega_c = 3\gamma$. Other values of parameters are the same as Fig. 3(a) except $\Delta_1 = \Delta_2 = 3\gamma$.

As mentioned above, the OB can be created via nonradiation coherence induced by the EPF in the present SQW system. Now we analyze how the EPF affects on the OB behavior. We show in Fig. 4(a) that the bistable threshold and the area of the bistable curve obviously decrease as the amplitude of the EPF Ω_c increases, which can also be chalked to the changes of absorption–dispersion property results from the increasing of Ω_c. By applying an increasingly intensity, the nonradiative coherence is enhanced. Thus, it is more easier for the absorption saturation of the ring cavity. In Fig. 4(b), we demonstrate that the bistable threshold reduces dramatically as C decreases. From the term $C = \frac{LN\omega_p\mu_{12}^2}{2\hbar c\varepsilon_0 T}$, it can be seen that C changes with N proportionally. Therefore, the decrease of the bistable threshold intensity origins from that the probe absorption of the sample enhances with the increasing of N. Besides, in the experimental application, the present SQW system can be engineered to obtain desirable dipole moments μ_{12} for changing the parameter C by appropriately designing the SQW sample.

As shown in Figs. 3 and 4, we have demonstrated the creation of the OB and studied the influences of parameters on the bistable behavior in the SQW system under consideration by fixing the phase difference between two components of polarized electric field (i.e. $\phi = 0$). However, we should examine the influence of the phase difference ϕ between two components of polarized electric field on the optical steady behavior, which is one of the most interesting characters of the present SQW system driven by the EPF. The phase of applied laser fields has been widely taken advantage of the coherent control of several vital processes in various SQW system.[23–35] Therefore, we present numerical results in Fig. 5 for examining the effect of the phase difference ϕ on the steady behavior. We show in Fig. 5 that the OB can be observed for $\phi = 0$ (solid line). More interestingly, one can find from Fig. 5 that the behavior of OM occurs as the phase difference ϕ increases from 0 to $\pi/3$ (dotted line). Furthermore, Fig. 5 also shows that the behavior of OM will

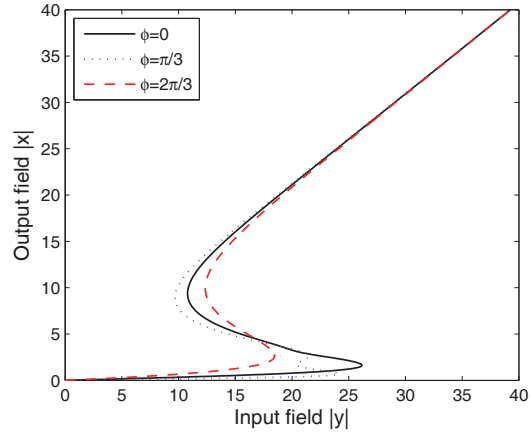

Fig. 5. (Color online) The curve diagrams of the input–output field intensity with different phase difference ϕ between two components of polarized electric field of the EPF with $\Delta_1 = \Delta_2 = 3\gamma$. Other values of parameters are the same as Fig. 3(a).

turn back to OB if ϕ is changed from $\pi/3$ to $2\pi/3$ (dashed line). The reason for the appearance of OM is that the nonradiation coherence is dependent on the phase difference ϕ, which implies that the absorption–dispersion property can be modulated by ϕ. The OM will appear so long as the input intensity $|y|$ in Eq. (15) is not a cubic polynomial of the output intensity $|x|$. Thus, we provide a alternative method for switching OB to OM or vice versa via tuning the phase difference between two components of polarized electric field of the EPF.

Before conclusion, the possible experimental realization of the present scheme is provided for creation of the controllable steady behavior in the SQW system. Experimentally, the SQW system presented here can be obtained at low temperature from a GaAs semiconductor sample in the current technology.[43] To obtain the two components of polarized electric field σ^+ and σ^- of the control field, one can let the control beam pass through a 1/2 and a 1/4 wave plates in turn properly. After passing the 1/2 wave plates, the vertical polarized beam can be obtained. The rotating angle ϕ can be modulated by the 1/4 wave plate. Thus, one can obtain that the elliptically polarized field contains two components (i.e. σ^+ and σ^-).

In conclusion, we have analyzed in detail the optical steady behavior in GaAs quantum well structure driven by an elliptically polarized field (EPF) in a unidirectional ring cavity. It is clearly shown that the controllable optical steady behavior including multi-stability (OM) and optical bistability (OB) can be obtained via nonradiation coherence, and the frequency detuning, cooperation parameter and the amplitude of the EPF can affect the bistable behavior effectively. Interestingly, our numerical results show that the conversion between OB and OM can be realized by adjusting the phase difference between two components of polarized electric field of the EPF. As a result, an alternative scheme for obtaining optimally the desired OM or OB provide a guidance in the design of an all-optical switch. In addition,

the present investigations of the optical steady-state behavior of the probe field in SQW system may open up a new gate for the applications of the nonradiative coherence.

Acknowledgments

The research is supported in part by National Natural Science Foundation of China under Grant Nos. 11374050 and 61372102, by Qing Lan project of Jiangsu, and by the Fundamental Research Funds for the Central Universities under Grant No. 2242012R30011.

References

1. H. M. Gibbs, S. L. McCall and T. N. C. Venkatesan, *Phys. Rev. Lett.* **36** (1976) 1135.
2. M. Kitano, T. Yabuzaki and T. Ogawa, *Phys. Rev. Lett.* **46** (1981) 926.
3. C. M. Savage, H. J. Carmichael and D. F. Walls, *Opt. Commun.* **42** (1982) 211.
4. A. T. Rosenberger, L. A. Orozco and H. J. Kimble, *Phys. Rev. A* **28** (1983) 2569.
5. H. J. Carmichael, C. M. Savage and D. F. Walls, *Phys. Rev. Lett.* **50** (1983) 163.
6. S. Singh, J. Rai, C. M. Bowden and A. Postan, *Phys. Rev. A* **45** (1992) 5160.
7. W. Harshawardhan and G. S. Agarwal, *Phys. Rev. A* **53** (1996) 1812.
8. S. Gong, S. Du, Z. Xu and S. Pan, *Phys. Lett. A* **222** (1996) 237.
9. Z. Chen, C. Du, S. Gong and Z. Z. Xu, *Phys. Lett. A* **259** (1999) 15.
10. X. Hu and Z. Xu, *J. Opt. B: Quantum Semiclass. Opt.* **3** (2001) 35.
11. A. Joshi and M. Xiao, *Phys. Rev. Lett.* **91** (2003) 143904.
12. H. Chang, H. Wu, C. Xie and H. Wang, *Phys. Rev. Lett.* **93** (2004) 213901.
13. A. Joshi, W. Yang and M. Xiao, *Phys. Rev. A* **68** (2004) 015806.
14. A. Joshi, W. Yang and M. Xiao, *Phys. Rev. A* **70** (2004) 041802(R).
15. J.-H. Li, X. Y. Lv, J. M. Luo and Q. J. Huang, *Phys. Rev. A* **74** (2006) 035801.
16. J. Wu, X. Y. Lv and L. L. Zheng, *J. Phys. B: At. Mol. Opt. Phys.* **43** (2010) 161003.
17. Z. Wang, A. X. Chen, Y. Bai, W. X. Yang and R. K. Lee, *J. Opt. Soc. Am. B* **29** (2012) 2891.
18. D. Zhang, J. Li, C. Ding and X. Yang, *Phys. Scripta* **85** (2012) 035401.
19. S. H. Asadpour and A. Eslami-Majd, *J. Lumin.* **132** (2012) 1477.
20. A. Joshi and M. Xiao, *Appl. Phys. B* **79** (2004) 65.
21. J. H. Li, *Phys. Rev. B* **75** (2007) 155329.
22. Z. Wang and H. Fan, *J. Lumin.* **130** (2010) 2084.
23. S. H. Asadpour, M. Jaberi and H. R. Soleimani, *J. Opt. Soc. Am. B* **30** (2013) 1815.
24. W. X. Yang, J. M. Hou and R. K. Lee, *Phys. Rev. A* **77** (2008) 033838.
25. W. X. Yang, J. M. Hou, Y. Y. Lin and R. K. Lee, *Phys. Rev. A* **79** (2009) 033825.
26. W. X. Yang, A. X. Chen, R. K. Lee and Y. Wu, *Phys. Rev. A* **84** (2011) 013835.
27. W. X. Yang, X. Yang and R.-K. Lee, *Opt. Express* **17** (2009) 15402.
28. W. X. Yang and R.-K. Lee, *Opt. Express* **16** (2008) 17161.
29. E. Paspalakis, M. Tsaousidou and A. F. Terzis, *Phys. Rev. B* **73** (2006) 125344.
30. J. H. Wu, J. Y. Gao, L. Selvestri, M. Artoni, G. C. La Rocca and F. Bassani, *Phys. Rev. Lett.* **95** (2005) 057401.
31. E. Paspalakis, A. Kalini and A. F. Terzis, *Phys. Rev. B* **73** (2006) 073305.
32. E. Paspalakis, *Phys. Rev. B* **67** (2003) 233306.
33. S. Ke and G. Li, *J. Phys.: Condens. Matter* **20** (2008) 175224.
34. G. Li, S. Ke and Z. Ficek, *Phys. Rev. A* **79** (2009) 033827.

35. D. Han, Y. Zeng and Y. Bai, *Opt. Commun.* **284** (2011) 4541.
36. J. M. Kikkawa, I. P. Smorchkova, N. Samarth and D. D. Awschalom, *Science* **277** (1997) 1284.
37. J. M. Kikkawa and D. D. Awschalom, *Phys. Today* **52** (1999) 33.
38. S. Sarkar, P. Palinginis, P.-C. Ku, C. J. Chang-Hasnain, N. H. Kwong, R. Binder and H. Wang, *Phys. Rev. B* **72** (2005) 035343.
39. P. Palinginis and H. Wang, *Phys. Rev. B* **70** (2004) 153307.
40. S. O'Leary, H. Wang and J. P. Prineas, *Opt. Lett.* **32** (2007) 569.
41. S. Crooker, D. Awschalom, J. J. Baumberg, F. Flack and N. Samarth, *Phys. Rev. B* **56** (1997) 7574.
42. P. Palinginis and H. Wang, *Phys. Rev. Lett.* **92** (2004) 037402.
43. H. Wang and S. O'Leary, *J. Opt. Soc. Am. B* **29** (2007) A6.
44. T. Li, H. Wang, N. H. Kwong and R. Binder, *Opt. Express* **11** (2003) 3298.
45. X. X. Yang, Z. W. Li and Y. Wu, *Phys. Lett. A* **340** (2005) 320.
46. J. B. Liu, N. Liu, C.-J. Shan, T. K. Liu and Y.-X. Huang, *Phys. Rev. E* **81** (2010) 036607.
47. U. Khadka, Y. P. Zhang and M. Xiao, *Phys. Rev. A* **81** (2010) 023830.
48. Y. Wu, M. G. Payne, E. W. Hagley and L. Deng, *Phys. Rev. A* **69** (2004) 063803.
49. Y. Wu, *Phys. Rev. A* **54** (1996) 4534.
50. Y. Wu and X. Yang, *Phys. Rev. A* **56** (1997) 2443.
51. R. Bonifacio and L. A. Lugiato, *Phys. Rev. A* **18** (1978) 1129.
52. P. Meystre, *Opt. Commun.* **26** (1978) 277.